

Supporting Information for
**Facile fabrication of nanofluidic diode membranes
using anodic aluminum oxide**

Songmei Wu, Fabien Wildhaber, Oscar Vazquez-Mena,
Arnaud Bertsch, Juergen Brugger, & Philippe Renaud

Microsystems Laboratory,
Ecole Polytechnique Federale de Lausanne (EPFL),
1015 Lausanne, Switzerland

Supplemental

1. Pattern transfer of local AAO mask into Si layer.

The porosity of the diode membrane can be modulated by plasma etching conditions and the thickness of the Si layer. The same etching conditions lead to higher porosity and larger pore diameters into thinner Si layer (Fig. S1).

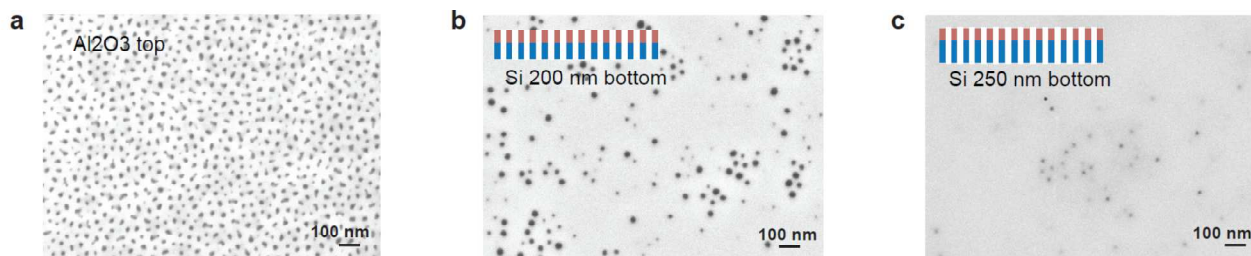


Fig. S1. Comparison of hetero-structured membranes obtained by 2 min of Cl_2 RIE into Si layers (with thickness of 200 nm and 250 nm) by using anodized alumina (original thickness of 220 nm) as mask. (a) top SEM image of alumina layer (remained thickness: 120 nm); (b) bottom SEM image of Si layer with thickness of 200 nm; (c) bottom image of Si layer with thickness of 250 nm.

2. Ag/AgCl electrodes and the cell constant.

The cell constant was measured in the liquid cell by using only the chip carrier after breaking the membrane. Compared to the conductivity measured by standard electrical conductivity meter, the home-made Ag/AgCl electrodes respond properly to various concentrations of KCl electrolyte. At concentrations below 0.01 mM, other impurity traces play important roles that the conductivity of the solution is similar to that of DI water (Fig. S2).

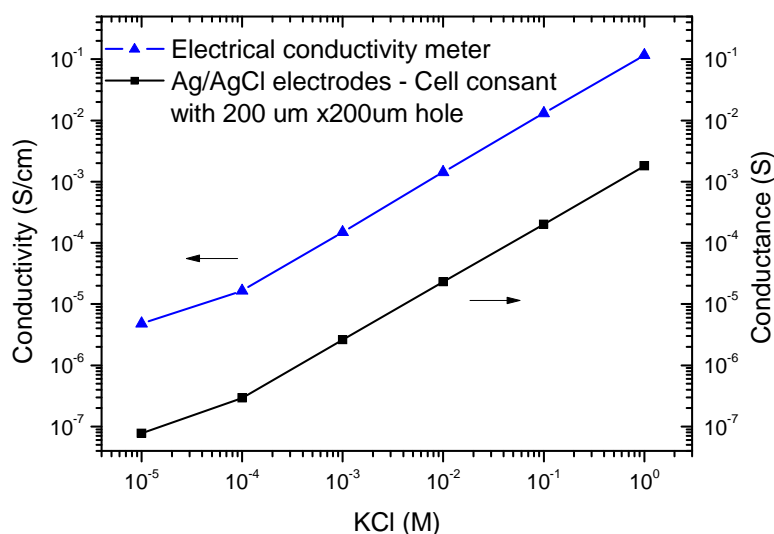


Fig. S2. Characterization of Ag/AgCl and the cell constant.

For a high porosity sample as shown in Fig. S1 b, the conductance of the membrane is larger or comparable to the cell constant so that only the cell constant can be observed.

3. Control experiments of mono-charged nanopore membranes.

Two control experiments were performed by using the devices with a) only bottom Si layer after dissolving top alumina layer in acid solution, and b) 5 nm alumina ALD coating. The rectification effect disappears because the channels possess only mono-charges. Typical I-V curves of a 5 nm alumina ALD coated membrane are shown in Fig. S3.

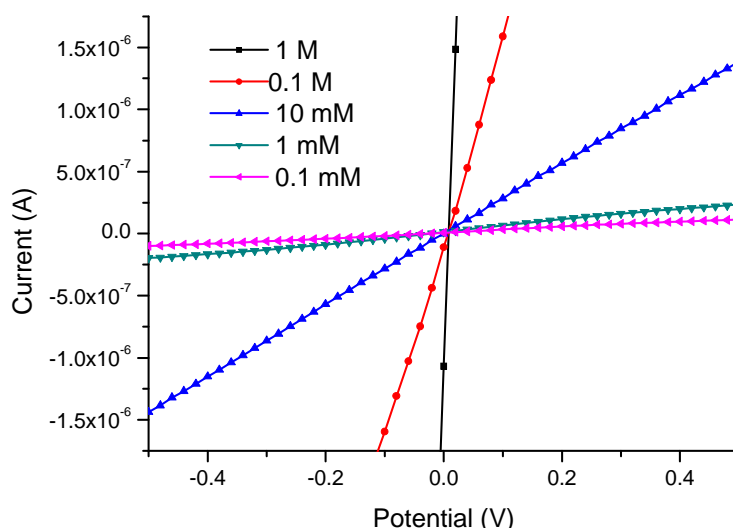


Fig. S3. Comparison of I-V curves obtained at varied KCl concentrations for a 5 nm Al_2O_3 ALD coated device.

Fig. S4 summarizes the conductance of mono-charged nanopore devices. A Si nanopore membrane has higher conductance values because the nanochannels are shorter. As for the ALD coated device, decreased porosity and pore diameters lead to lower conductance and eventually deviates from linear dependence of varied electrolyte concentrations.

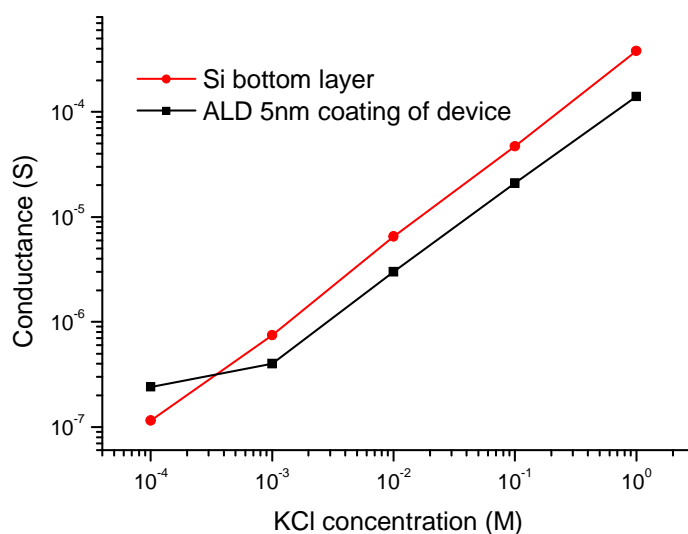


Fig. S4. Summarized conductance of mono-charged nanopore devices obtained by dissolving alumina layer of hetero-structured nanopore membrane or coating the entire device with 5 nm alumina by ALD.

4. Simulation of ionic transport in nanofluidic diodes

Fig. S5 shows schematically the considered nanofluidic device with axis-symmetrical geometry. It is a single nanopore (radius r_{pore} , and height h_{pore}) composed of two surfaces with opposite charge polarities ($\sigma_{\text{up}} = -\sigma_{\text{down}}$, with $\sigma_{\text{up}} > 0$). The surface area around the nanopores possesses similar charge polarity and density as those in corresponding internal walls of the nanopores. The nanofluidic diode channel is connected to two large reservoirs (radius r_{bulk} , and height h_{bulk}) filled with ionic solutions (C_{bulk}). The electrical potential was fixed to $-V_{\text{bias}}/2$ and $+V_{\text{bias}}/2$ at the top and bottom bulk boundaries (with this sign convention a positive value for V_{bias} corresponds to a forward bias and negative value to a reverse bias).

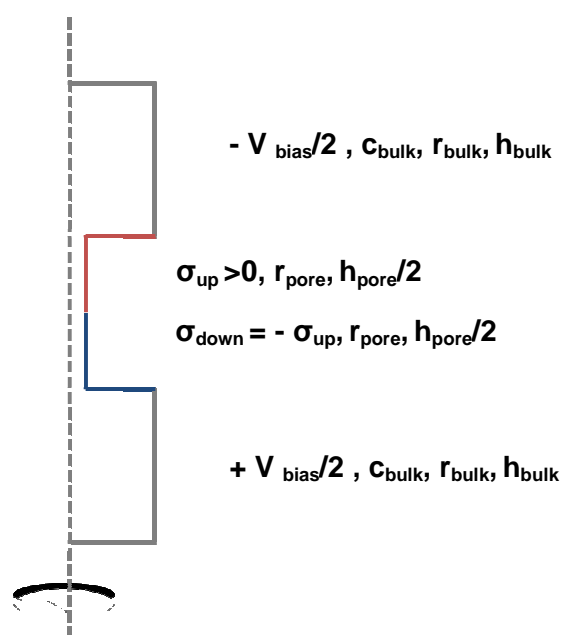


Fig. S5. Schematic of a single nanofluidic diode of radius r_{pore} and height h_{pore} connected to two reservoirs. The nanopore is composed of two surfaces with opposite charge polarities ($\sigma_{\text{up}} = -\sigma_{\text{down}}$). The surface area around the nanopores possesses similar charge polarity and density as those in corresponding internal walls of the nanopores.

The distribution of cations and anions and the electrical potential in the nanofluidic diode are described by the Poisson-Nerst-Planck equations:

$$\text{Poisson equation:} \quad \epsilon \Delta V = -\sum_i F z_i c_i \quad \text{equ.S.1}$$

$$\text{Nernst-Planck equation (without convection):} \quad \mathbf{N}_i = -D_i \nabla c_i + z_i u_i F c_i \nabla V, \quad \text{equ.S.2}$$

where ϵ is the dielectric constant of water, V the electric potential, F the Faraday constant, z_i the valence of the ion i , c_i the concentration, \mathbf{N}_i the molar ionic flux, D_i the diffusion constant and u_i the mobility. We restrained our study to the KCl electrolyte with cation K^+ and anion Cl^- .

The parameters were set to the following values: $D_{K^+} = 1.957 \times 10^{-9} \text{ m}^2/\text{s}$, $u_{K^+} = D_{K^+}/(RT)$, $T = 298\text{K}$, $z_{K^+} = +1$, $D_{Cl^-} = 2.032 \times 10^{-9}$, $u_{Cl^-} = D_{Cl^-}/(RT)$, $z_{Cl^-} = -1$, $h_{pore} = 400 \text{ nm}$, $r_{pore} = 10 \text{ nm}$, $h_{bulk} = 500 \text{ nm}$, $r_{bulk} = 200 \text{ nm}$, $c_{bulk} = 1 \text{ mM}$, $\sigma_{up} = -\sigma_{down} = 5 \text{ mC/m}^2$, $V_{bias} = 1 \text{ V}$, -1V respectively.

These equations were solved numerically by using the software COMSOL Multiphysics and coupling the modules Electrostatics and Transport of Diluted Species on the Vega Cluster at the center for High Performance Computing at EPFL.

By using a stationary solver, the steady state distribution of the cation concentration c_{K^+} and anion c_{Cl^-} concentration as well as the electrical potential V can be obtained as shown in Fig. S6, S7 and S8 for a zero, forward and reverse bias respectively.¹

The current flowing through the pore was derived from the concentration and voltage values by integration over a pore cross-section of the total ionic flux of both ions through it. The fact that the system is at steady-states guarantees that the ionic flux through the pore is a constant for any cross-section.

$$I = \int_{S=\text{Arbitrary CrossSection}} [z_{K^+} F(-D_{K^+} \frac{\partial c_{K^+}}{\partial z} - z_{K^+} u_{K^+} F c_{K^+} \frac{\partial V}{\partial z}) + z_{Cl^-} F(-D_{Cl^-} \frac{\partial c_{Cl^-}}{\partial z} - z_{Cl^-} u_{Cl^-} F c_{Cl^-} \frac{\partial V}{\partial z})] dS \quad \text{equ. S.4}$$

¹ The values plotted are the average $\bar{f}(z)$ over the pore cross-section of the function $f(r,z)$ at coordinate z , defined by

$$\bar{f}(z) = \frac{2\pi \int_{r=0}^{r_{pore}} r \cdot f(r,z) \cdot dr}{\pi r_{pore}^2}, \quad \text{where } f(r,z) \text{ is the concentration of chloride, of potassium, or the potential,}$$

respectively. The integration is performed between 0 and r_{pore} also in the reservoirs.

Fig. S6 describes the situation of zero bias. Since the pore is composed of two half-part with opposite surface charges the ionic concentrations are symmetrical for the two sides of the nanopore. At steady state no net flow of ions occurs, which means that the diffusion flux compensates exactly the migration flux at every point in the channel. The simulation shows a ten-fold accumulation of counter-ions and a ten-fold depletion of co-ions on both sides of the pore compared to bulk ionic concentration, and the electrical potential is bent by the accumulation of charges via the Poisson law.

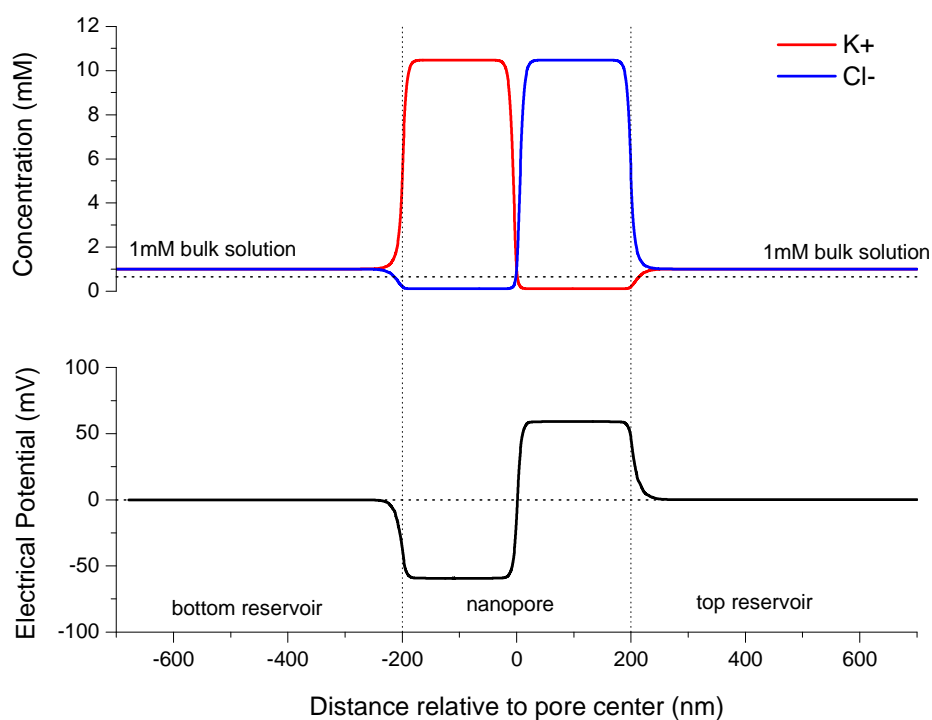


Fig. S6. Concentration profile of potassium and chloride ions and potential distribution through the device at zero bias. The accumulation of counter-ions and depletion of co-ions occur on both sides of the nanopore.

The distribution of ions changes dramatically in the nanopore when a forward bias is applied through the bottom and top side of the reservoir. As illustrated in Fig. S7, both positive and negative ions accumulate on both co-charged and counter-charged sides reaching a 60-fold accumulation at the center of the pore. The applied potential at the boundary induces a steady-state flux of ion through the pore, resulting in ionic current at 1 V forward bias $I_{fwd} = 217.42$ pA according to equ.S.4.

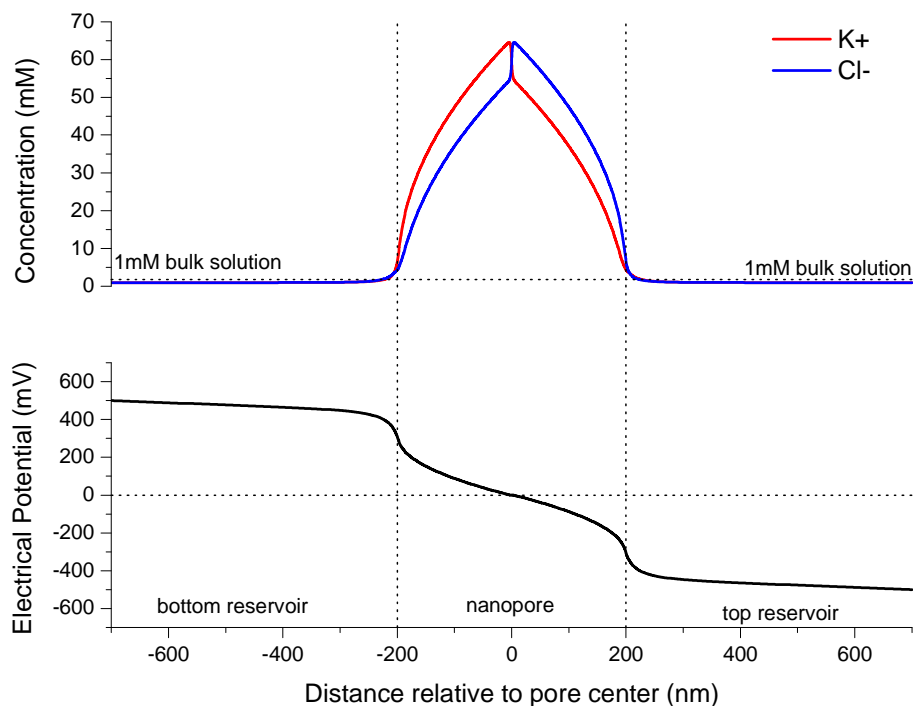


Fig. S7. Concentration profile of potassium and chloride ions and potential distribution through the device at 1 V forward bias. Both counter-ions and co-ions accumulate towards the center of the nanopore.

In the case of a reverse bias (Fig. S8), The depletion effect is further extended than the situation of zero bias. The steady-state current at 1 V backward bias is $I_{bwd} = 0.07$ pA obtained via equ.S.4 which is about 3 orders of magnitude lower than the current at forward bias.

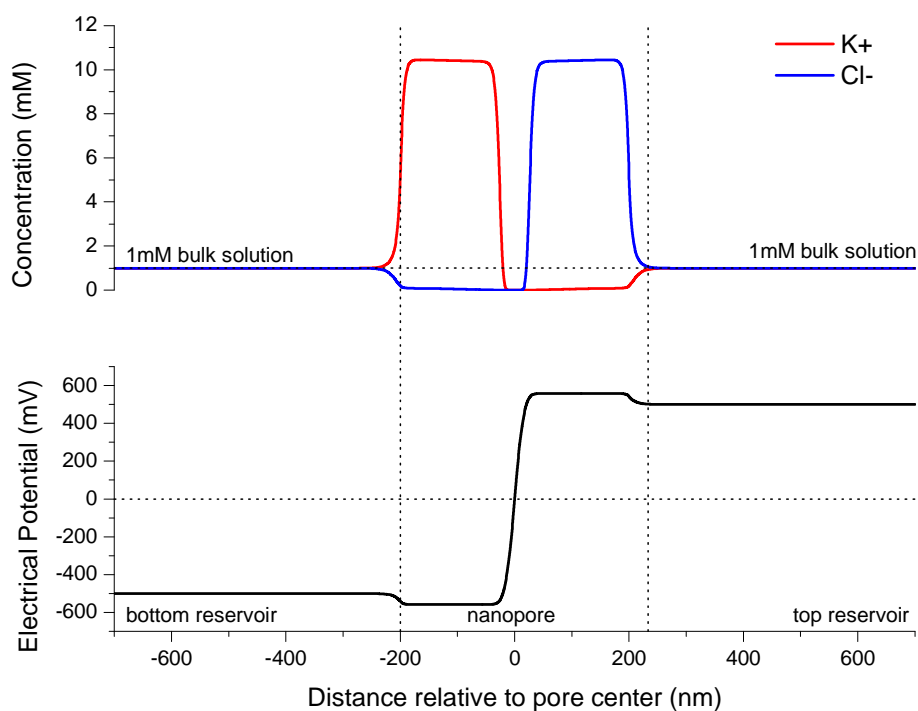


Fig. S8. Concentration profile of potassium and chloride ions and potential distribution through the device at 1 V reverse bias. A depletion zone of both counter-ions and co-ions is built at the center of the nanopore.